Bulletin of the Seismological Society of America, Vol. 106, No. 4, pp. 1509–1517, August 2016, doi: 10.1785/0120160004

A Study on Kappa Value in Taiwan Using Borehole and Surface Seismic Array

by Tz-Shin Lai,* Himanshu Mittal, Wei-An Chao, and Yih-Min Wu†

Abstract Since the inception of the borehole seismic array deployed by the Central Weather Bureau (CWB) in Taiwan in recent years, a large quantity of strong-motion records have been accumulated from frequently occurring earthquakes around Taiwan that provide the opportunity to investigate the spectral decay parameter kappa (κ) and to understand further the site effects of seismic stations. In this study, we used 133 earthquakes recorded at 30 borehole seismic arrays. Each array includes two force-balance accelerometers, one at the surface and the other inside the borehole. Based on the regression analysis between κ-value and hypocentral distance for each surface–borehole station pairs, the resulting κ_0 derived from surface stations are higher than results from borehole stations. The estimated κ_0-values are found to range from 0.032 to 0.097 s at surface and 0.012 to 0.078 s in borehole. In comparison with a study of site corrections for earthquake magnitude determination, these higher κ_0-values associated with negative station corrections can correspond to the effect of soil conditions. To evaluate station corrections of borehole seismic array, we collected records from the cosite stations of Taiwan Strong-Motion Instrumentation Program (TSMIP) and Central Weather Bureau Station Network (CWBSN) and then derived a linear relationship between the κ_0-values and station corrections. Finally, both resulting station corrections and κ_0-values reveal high coherence in local site conditions.

Introduction

Ground-motion prediction equations (GMPEs) are statistical models to predict ground-shaking parameters (peak ground acceleration, peak ground velocity, spectral acceleration) as a function of source, site, and path-effect parameters like magnitude, faulting pattern, epicentral distance, and site conditions. As seismic waves travel from source to recording stations, their amplitude and frequency gets changed. They get attenuated or amplified according to propagation path as well as site conditions. Attenuation in seismological studies can be described as decay of amplitude with distance. High-frequency spectral decay consists of all three factors, namely source, site, and path. In the 1980s, it was observed that attenuation of high-frequency spectra cannot be explained using whole-path attenuation (Ktenidou *et al.*, 2013). The amplitude of the spectrum increases until it reaches corner frequency (f_0). Beyond f_0, the shape of the spectrum is defined in different ways.

Hanks (1982) first proposed the concept of high-end cutoff frequency $f_{\max}$ and stated that the spectrum is flat from corner frequency to $f_{\max}$. Above $f_{\max}$ the acceleration spectrum decays rapidly as

$$[1 + (f/f_{\max})^8]^{-\frac{1}{2}}. \tag{1}$$

Hanks (1982) related the concept of $f_{\max}$ to site effects, whereas later Papageorgiou and Aki (1983) related this observation to source effect. The rate of decay of strong ground motion at higher frequency introduced by Anderson and Hough (1984) can be represented exponentially by the following relation:

$$A(f) = A_0 \exp(-\pi\kappa f), \quad f > f_e, \tag{2}$$

in which κ is the spectral decay parameter that accounts for attenuation of seismic waves, f_e is a frequency above which the decay is assumed to be linear, and A_0 is a source and propagation path-dependent amplitude.

Using the least-squares fitting method, values of κ can be estimated from the slope λ of the acceleration spectrum (a) over a range of frequencies (Δf), using the following relation:

$$\kappa = -\lambda/\pi, \quad \lambda = \triangle(\ln a)/\triangle f. \tag{3}$$

κ is a very important parameter in the stochastic technique used for generation of strong ground motion in areas not

*Now at Seismological Observation Center, Central Weather Bureau, Taipei 10048, Taiwan.

†Also at National Center for Research on Earthquake Engineering, NARLabs, Taipei 10668, Taiwan.

having much recorded strong-motion data to enable the derivation of robust empirical GMPE.

A relation between κ and epicentral distance $R(s)$ of the recording station was observed by Anderson and Hough (1984). They proposed a linear relationship between the intercept of the κ trend with distance (denoted κ_0) and shear-wave attenuation through the subsurface, whereas the slope (κ_R) refers to attenuation through the crust. The relation is given by

$$\kappa = \kappa_0 + \kappa_R \times R(s), \tag{4}$$

in which κ_0 is the factor accounting for attenuation due to near-surface geology and is specific to each site, and κ_R refers to distance dependence of κ, set to be zero at epicenter (Anderson, 1991). According to Anderson and Hough (1984), κ_R is related to the seismic quality factor Q.

Despite being such an important factor in high-frequency wave modeling, the existence and dependence of κ on various factors such as source, site, and path is highly debatable. The initial studies (Hanks, 1982; Anderson and Hough, 1984) stated that the existence of κ proposed high-frequency decay as a site parameter, whereas the other studies recognized it to be related to source effects (e.g., Papageorgiou and Aki, 1983). However, recent studies (Tsai and Chen, 2000; Purvance and Anderson, 2003) suggested that high-frequency decay factor values may be related to both site as well as source components. In most of the works, κ is considered to be path- and site-dependent (e.g., Hough and Anderson, 1988; Hough *et al.*, 1988; Anderson, 1991; Campbell, 2009; Fernández *et al.*, 2010; Ktenidou *et al.*, 2013).

Many studies related to κ-value have been performed around the world (e.g., Margaris and Hatzidimitriou, 2002; Cotton *et al.*, 2006; Oth *et al.*, 2010; Lancieri *et al.*, 2012). κ-value is not only a useful parameter in establishing GMPE for a particular region, but also is important in stochastic ground-motion simulation methods to limit the attenuation and spectral shape of synthetic seismogram (e.g., Boore, 2003; Motazedian and Atkinson, 2005; Mittal and Kumar, 2015; Mittal *et al.*, 2016). Ktenidou *et al.* (2013) estimated κ-values from the Greek Corinth Soft Soil Array (CORSSA) consisting of five accelerometers at different depths. They calculated depth-dependent κ_0-value to understand the site effects and geologic characteristics of the ground stations. In Taiwan, there are only a few studies related to κ-values. Tsai and Chen (2000) proposed an alternative model in which they stated that κ depends mainly on the source, on site to some extent, and on distance only a little bit. They used accelerograms observed at stations of the Strong Motion Array Taiwan (SMART 1 array) to establish a regression formula to obtain an estimate of f_e and κ in a local area. Van Houtte *et al.* (2011) illustrated the distance dependence of κ at the surface, with a resulting κ_0-value of 0.05 for the Taiwan region. Chen *et al.* (2013) used a total of 90 events recorded by the portable seismic array during the period from 1995 to 1997 to estimate κ_0-value distribution in the the Kaoping area in southwestern Taiwan, which confirms the distribution of sediment thickness. The above-mentioned studies only investigated the κ-value in the specific region as well as the average κ_0-value for the Taiwan region. Recently, the borehole seismic array has been deployed by the Central Weather Bureau (CWB) and well distributed in Taiwan. It provides a good opportunity to systematically analyze the high-frequency spectral-amplitude decay by determining κ using both surface and borehole records and by comparing them for the entire Taiwan region. This study to determine κ using borehole records is the first of its kind in Taiwan. According to Anderson and Hough (1984), we assume the κ_0-value in equation (4) is corresponding to a site effect in the present work.

Study Area and Dataset

The area studied is Taiwan, which is located on the western Circum-Pacific seismic belt. It is perhaps one of the most seismically active regions in the world, due to the collision of the Eurasian plate (EP) and the Philippine Sea plate (PSP). Toward the east, PSP subducts northward beneath the EP, and toward south the EP subducts eastward under the PSP. The suture zone between PSP and EP divides Taiwan into two tectonic regions. To improve the accuracy of earthquake location and regional monitoring capacity of small-scale earthquakes in Taiwan, CWB in recent years built a high-quality deep-seismic observation stations array. By the end of 2013, this amounted to a total of 30 seismometers in the array, that is, surface–borehole seismic instruments have been installed in different parts of the country. Each station pair has a three-component force-balanced accelerometer (FBA)-type seismograph at the surface and two downhole instruments, that is, velocity-type broadband and FBA-type seismometers. We choose to work with data from surface-downhole accelerometers only. These FBA sensors have a high sampling rate of 200 Hz. The underground instruments are placed at a depth between 120 and 400 m, which one can imagine is almost to the depth of the bedrock. Some of the stations have site characterization available through various deep-drilling sampling records and core data. In this study, we use these valuable borehole seismic-array data to investigate site effects and offer information for the estimation of earthquake magnitude, including borehole stations in the future. We use surface and downhole acceleration waveform data from 133 earthquakes, from 1 January 2012 to 31 December 2013, having local magnitude (M_L) more than 4 and focal depth less than 35 km (Fig. 1). These earthquakes have been well relocated by the location method of Wu *et al.* (2008), using the recent 3D velocity model of Wu *et al.* (2007) in Taiwan.

Data Processing

For each record in our dataset, the three-component waveform data are baseline corrected. We then manually pick up arrival times of P and S waves. A five-second-length time window in the pre-event part before the time point of

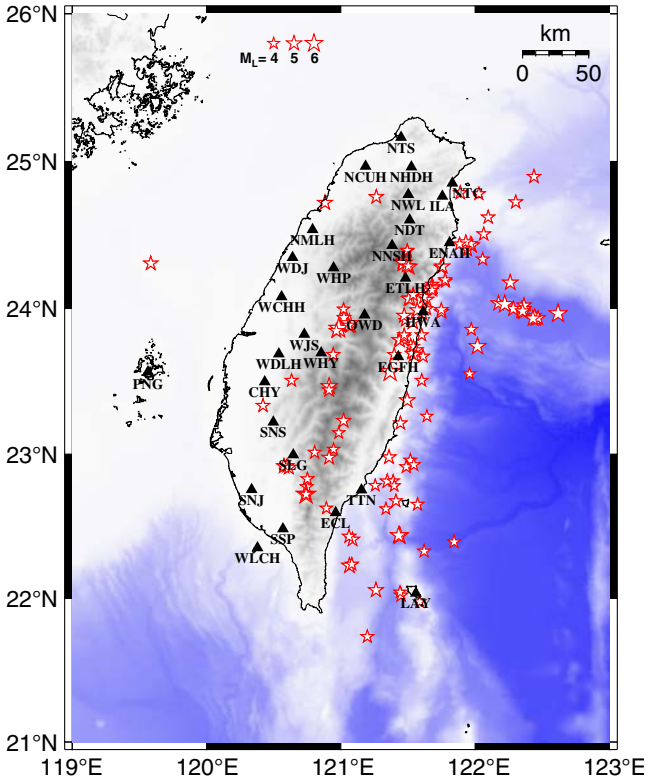

Figure 1. Epicenter distribution of 133 earthquakes used in this study. The sizes of the stars are proportional to the magnitude. Distribution of borehole seismic arrays is shown by triangles. The color version of this figure is available only in the electronic edition.

P-wave arrival is taken as background noise, whereas a five-second-length window (0.5 s before *S*-wave arrival and 4.5 s after *S*-wave arrival) is taken as signal. The manually determined *P* and *S* arrivals from the horizontal-component (east–west and north–south) accelerograms recorded at CHY station for the M_L 6.2 event at an epicentral distance of 78 km are shown in Figure 2. The average amplitude in the *S*-wave window is divided by the average noise level to calculate the signal-to-noise ratio (SNR). Only waveforms with an SNR larger than 100 are used in our study. Then, the *S*-wave waveforms are transformed to a frequency domain using the fast-Fourier transform approach. We only utilize the acceleration spectra with sufficient spectra SNR (>3) to perform the κ-value analysis. Before calculating spectral SNR value, smoothing was performed for *S*-wave and noise-window spectra with a mild Konno–Ohmachi filter (Konno and Ohmachi, 1998) and equally distributed to a common frequency step of 1-Hz window length. The acceleration spectra are checked in log–linear space to find the values of frequencies f_e and f_x. The frequency band $\Delta f = f_e - f_x$ is adjusted to have a spectral SNR > 3 (Fig. 3). Spectra having $\Delta f < 10$ Hz are not considered to compute slope in an efficient way. Depending on the magnitude and distance of the event, the value of frequency f_e is found to range from 2 to 15 Hz, whereas f_x lies between 11 and 50 Hz. Here, we get large-frequency range for κ computation, as the Nyquist frequency based on the sampling rate is 100 Hz. The selected frequency range for each accelerogram spectrum is used to estimate the linear trend of decay in spectral amplitude. Using equation (3), the value of κ is calculated for all four components, that is, two at surface and two downhole for each event, based on the slopes of the spectra. The average κ-values for each event-to-station pair were computed from the resulting κ-values on horizontal-component spectra. Only the average κ-values with a range of ratio from 0.5 to 2.0, which is calculated from the ratio of resulting

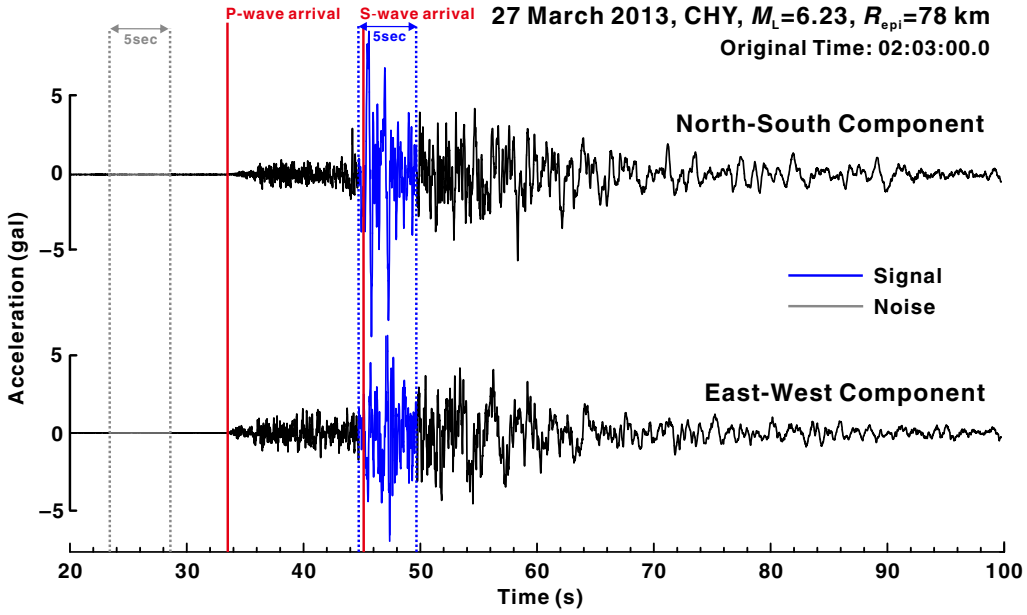

Figure 2. The selection of signal window as well as noise window after manual picking of *P* wave and *S* wave. The color version of this figure is available only in the electronic edition.

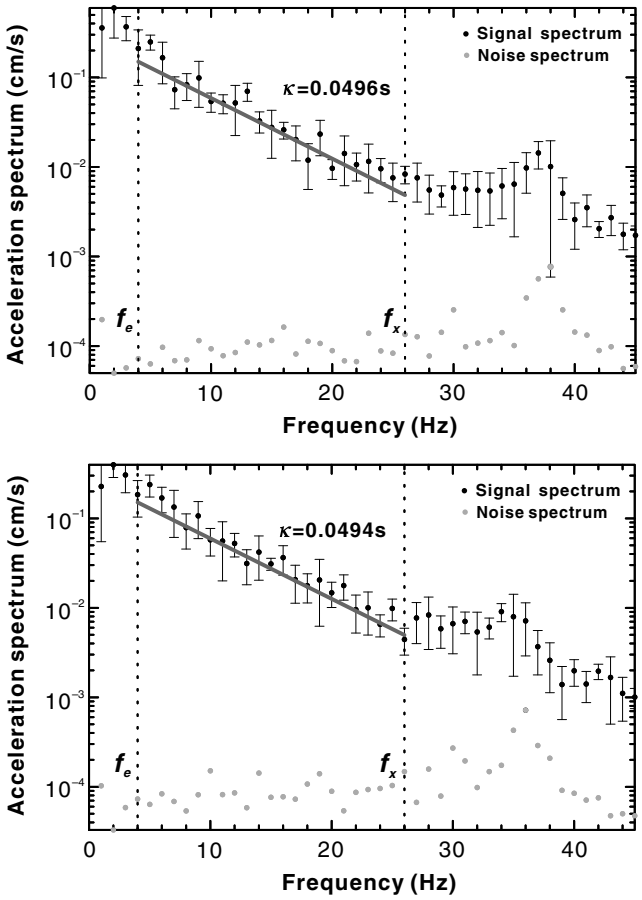

Figure 3. κ-value calculation process using the north–south and east–west component of the CHY underground station. The dark point represents a signal amplitude spectrum, whereas the gray point gives a noise amplitude spectrum. Values of f_e and f_x are picked, and κ-value is calculated using the least-squares (LS) method, resulting in (upper) 0.0496 in the north–south direction and (lower) 0.0494 in the east–west direction.

κ-values between the north–south-component and east–west-component spectra, were used in the κ_0 computation. In a case of Figure 3, the ratio of resulting κ-values is about 1.004. The flowchart for κ computation is shown in Figure 4.

κ_0 Computation

Once the κ-value is estimated for each event and station pair, we further estimate the value of near-surface attenuation parameter κ_0 according to equation (4) as proposed by Anderson and Hough (1984). Here, two-stage inversion procedures have been adopted for the estimation of κ_0-value. In the first stage, we found a linear relationship between κ-value and hypocentral distance by the conventional least-squares (LS) method (dashed line in Fig. 5a) that minimizes the sum of squared errors of all points from the line. Next, we define a weighting coefficient based on a function of $0.1/(0.1 + |\Delta r|)$. Δr is the vertical misfit between the resulting regression line and data point. Second, we conducted

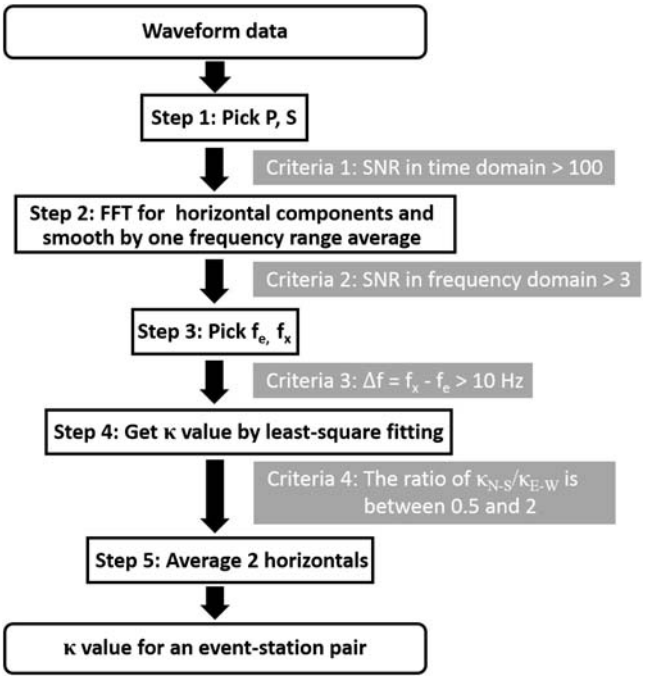

Figure 4. A flowchart showing the step-by-step procedure of the κ calculation.

weighted LS method through a grid-search scheme for ranges of slope and intercept (κ_0) from 10^{-5} to 10^{-3} and 0 to 0.15, respectively. After three iterations, optimal and reliable κ_0-values are obtained from weighted LS, which significantly improve the robustness of regression analysis (solid line in Fig. 5a).

Results and Discussion

Dependence of κ on Distance

After estimation of κ-value for each event-to-station pair, we check the dependence of κ-value on distance using equation (4). Anderson and Hough (1984), who proposed the concept of κ, used epicentral distance in their study. There is no clear indication as to which distance should be used. Some researchers (e.g., Douglas *et al.*, 2010; Ktenidou *et al.*, 2013) use epicentral distance, whereas others (e.g., Castro *et al.*, 2000; Van Houtte *et al.*, 2011) use hypocentral distance. The use of hypocentral distance looks more appealing, because it is closely related to the path followed by seismic waves from source to site. Some consider epicentral distance to be more useful, because the main point of computation is to calculate κ_0, which can be obtained by extrapolating κ_R to $R = 0$. This cannot be achieved using hypocentral distance, which cannot be zero until the depth equals zero. However, because we are using crustal earthquakes (focal depth < 35 km), we think that either hypocentral or epicentral distance has no obvious influence in our results. Indeed, for an example of CHY station at the surface, using the epicentral distance in regression analysis

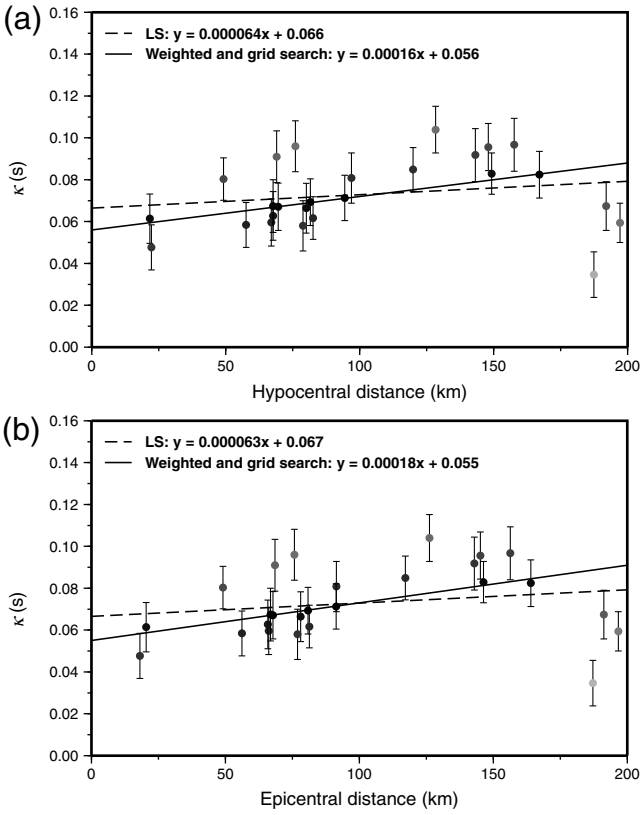

Figure 5. Distributions of κ-value with (a) hypocentral distance and (b) epicentral distance for the CHY station placed at surface. The dashed and solid lines show the regression results using the LS method only and weighted LS through a grid-search scheme (two-stage inversion). Resulting κ_0-values of LS and two-stage inversion for using hypocentral distance are 0.066 and 0.056, respectively. For the case of epicentral distance, resulting κ_0-values of LS and two-stage inversion are 0.067 and 0.055, respectively.

of equation (4), there is only ~2% difference in the resulting κ_0-value. Thus, the hypocentral distance was used in the above-mentioned κ_0 computation. Figure 6 shows a κ_0-value at the same station in the borehole is 0.030, which is less than the resulting κ_0 at the surface (termed κ_0^s). Detailed discussion can be found in the next section.

Surface and Borehole κ-Value

Figure 7a shows the distribution of κ_0^s-value. The seismic stations located in the western plains (NMLH, WHP, WJS, CHY, SNS, and SSP), Lanyang plain (ILA and NTC), and basin (NHDH), which are rich in alluvium, show relatively large κ_0^s-values ($\kappa_0^s > 0.05$), implying that attenuation of seismic waves is faster. On the other hand, the stations located in mountains (NWL, NDT, ENAH, NNSH, ETLH, OWD, EGFH, SLG, and ECL) show smaller κ_0^s-value ($\kappa_0^s < 0.05$), displaying near-surface attenuation to be low. From here it can be inferred clearly that κ_0^s and the station geology are closely related.

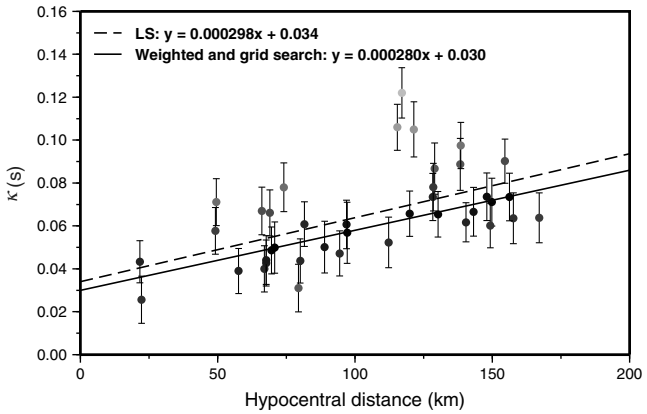

Figure 6. Distribution of κ-value with hypocentral distance for the CHY station placed in borehole. The value of κ_0 derived by two-stage inversion procedures is found to be 0.030. The dashed line indicates the regression line determined by the LS method only in resulting the κ_0-value of 0.034.

On studying the distribution of κ_0-value (termed κ_0^b) for borehole stations (Fig. 7b), it is inferred that the stations located in mountains (NWL, NDT, NNSH, OWD, EGFH, WHY, and SLG) exhibit lower κ_0^b ($\kappa_0^b < 0.04$). However, for stations located in other regions (NHDH, ILA, HWA, TTN, LAY, NMLH, WDJ, WHP, WCHH, WJS, CHY, SNS, SSP, and WLCH), no regular pattern is observed related to depth of instruments (200–400 m) or thickness of alluvium. The change in κ_0^b-value at different stations may be attributed to geologic environment. Table 1 depicts the calculated values of κ_0^s and κ_0^b for all the stations. Only 16 stations are listed in Table 1 because the number of data points (<3 points) for some stations was not sufficient for regression analysis to find the value of κ_0^s and κ_0^b.

The results of this study are compared with previous studies in Taiwan to check the credibility. In our study, we found an average value of κ_0^s to be 0.05, which is consistent with the result of Van Houtte *et al.* (2011). Chen *et al.* (2013) found high κ_0^s-value in the Pingtung area as compared to other regions in Taiwan, suggesting high attenuation. High κ_0^s-values are also obtained in present study in the Pingtung area as compared to other regions, which is in rough agreement with a previous study.

Relation between κ_0^s and κ_0^b

As most of the borehole stations are located at a range of depth from 200 to 400 m, the seismic waves that reach the borehole stations are less attenuated related to the surface stations, for which the high-frequency seismic amplitudes rapidly decay, resulting in higher κ_0^s-values. Figure 8 shows the comparison between κ_0^s- and κ_0^b-values. The value of κ_0^s is generally larger than the κ_0^b-value. Only a few studies have been carried out to find a relation between κ_0^s and κ_0^b. Oth *et al.* (2011) used a Japanese networks dataset to find a possible relation between surface and borehole κ-values at

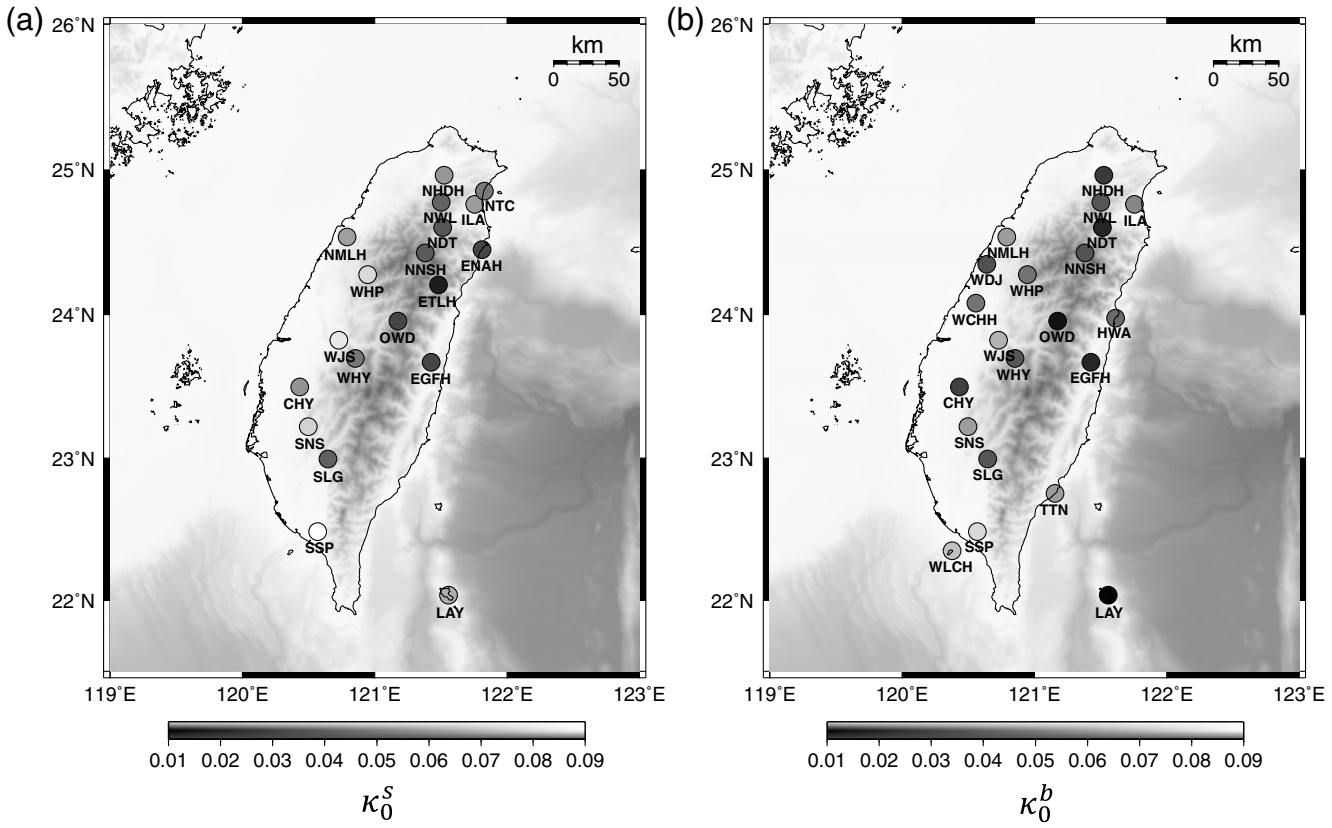

Figure 7. Distribution of κ_0-value (a) at surface stations and (b) in borehole stations.

different depths as a function of site effects, and they also found the mean of surface κ-value is larger than borehole κ-values. Path correction was applied before computation. Van Houtte *et al.* (2011) computed κ_0-values for surface and borehole stations as a function of distance and reported larger κ_0 at surface than borehole.

Table 1
κ_0^s- and κ_0^b-Values for Different Stations Using Two-Stage Inversion Procedure

Station	Longitude (°E)	Latitude (°N)	Elevation (m)	κ_0^s (s)	κ_0^b (s)
CHY	120.4325	23.4963	398	0.056	0.030
EGFH	121.4274	23.6688	295	0.032	0.022
ILA	121.7563	24.7638	177	0.059	0.052
LAY	121.5581	22.0373	196	0.065	0.012
NDT	121.5128	24.6025	200	0.037	0.022
NHDH	121.5250	24.9630	210	0.057	0.028
NMLH	120.7910	24.5372	296	0.060	0.059
NNSH	121.3829	24.4284	293	0.038	0.036
NWL	121.5025	24.7772	197	0.041	0.037
OWD	121.1759	23.9545	290	0.032	0.016
SLG	120.6463	22.9934	350	0.040	0.037
SNS	120.4973	23.2198	300	0.076	0.059
SSP	120.5681	22.4835	295	0.097	0.078
WHP	120.9458	24.2777	122	0.078	0.046
WHY	120.8532	23.6961	300	0.047	0.037
WJS	120.7279	23.8219	292	0.083	0.066

Relation between $\Delta\kappa_0$ and Surface-to-Borehole Distance

We tried to study the possible relationship between differences of κ_0-value ($\Delta\kappa_0$) for each station pair (surface-to-borehole) with corresponding vertical distance of surface-to-borehole. The results are plotted in Figure 9, and there is no obvious correlation between $\Delta\kappa_0$ and surface-to-borehole distance. In fact, the $\Delta\kappa_0$-value is entirely related to the geologic material in which instruments are placed. For instance, the surface-to-borehole distance of the LAY station is 196 m. From drilling sampling at this site, it is found that the upper 2.5 m layer is sedimentary, whereas at 2.5–196 m it is andesite rock. Therefore, the difference of geology makes the $\Delta\kappa_0$-value be the largest up to 0.053 in the LAY station. In contrast, the surface-to-borehole distance of the CHY station is 398 m, but there is a relatively small $\Delta\kappa_0$-value of 0.026, because the site of the station is on sediment. More details about drilling core records are needed to fully understand the relation between $\Delta\kappa$ and the vertical distance of surface-to-borehole for each station pair.

Relation between Station Correction of M_L and κ_0-Value

Station correction of M_L was studied at 142 stations in one of the earlier studies (Lai *et al.*, 2016) using data from

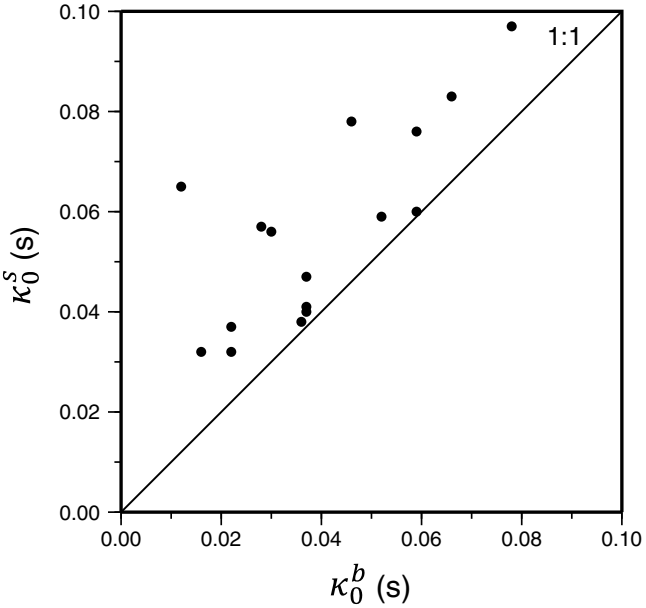

Figure 8. Comparison of κ_0^s- and κ_0^b-values.

1994 to 2014 recorded by Geotech S13 short-period seismometers from the Central Weather Bureau Station Network (CWBSN) (CWBSN-S13). To estimate the station corrections and revise the magnitude, data from the CWBSN earthquake catalog were analyzed. For each earthquake, magnitude difference (ΔM_L) is calculated between the earthquake magnitude (M_L) and the station magnitude (M_L^S) for each station. The mean value of the total magnitude differences (ΔM_L) at a particular station is defined as station correction of that station. A strong correlation is found between station corrections and geologic settings of the region. Stations located on soil sites have high amplifications with negative station corrections. On the other hand, stations located on hard-rock sites have low amplifications with positive station corrections. In comparison with a study of site corrections, higher κ_0-values associated with negative station corrections can correspond to the effect of soil conditions. We try to study the possible relation between station correction of M_L and κ_0-value. Because both these studies are performed using different stations, we located stations from the Taiwan Strong-Motion Instrumentation Program (TSMIP) network, which are at the same site as that of CWBSN-S13. Consequently, we find 16 cosite stations. At all 16 TSMIP stations having FBA-type accelerometers, κ-values are estimated using available accelerograms. After calculation of κ-value, κ_0-values are estimated using two-stage inversion procedures as described in the κ_0 Computation section. The stations located in the plains, which are rich in alluvium, show relatively large κ_0-value as compared to the stations located in mountains. Table 2 gives estimated κ_0 at all cosite TSMIP stations along with station correction of M_L. The distribution of κ_0-values is in agreement with the results derived from the borehole seismic array (Fig. 10). Furthermore,

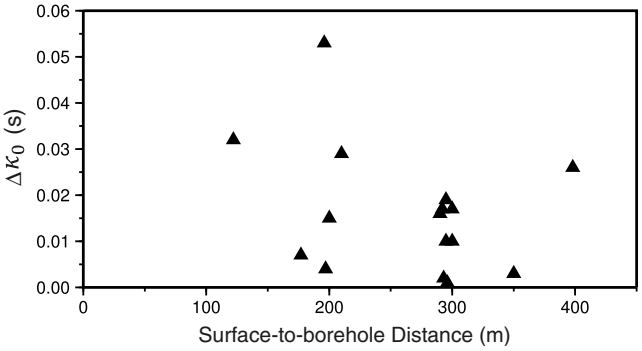

Figure 9. $\Delta\kappa_0$ values as a function of surface-to-borehole distance.

regression analysis is performed between station correction of M_L and κ_0-value to find their relationship. As seen from Figure 11, for positive station correction, lower values of κ_0 are observed. In contrast, for negative station correction, higher value of κ_0-values are observed. The result of the regression allows for simple determination station corrections of the borehole seismic array with large uncertainty, by inputting the estimated κ_0-values. Because standard deviation is very high, this relation does not provide direct information about parameters; however, it provides another indirect evidence of site dependence of the estimated κ_0-values with the site-specific geologic conditions.

Conclusions

In the present work, we applied a robust method of two-stage inversion to determine κ_0-values in Taiwan from 30 borehole seismic arrays containing FBA accelerometers at surface and borehole. We explore the importance of includ-

Table 2
List of Cosite TSMIP and CWBSN-S13 Stations along with κ_0 and Station Correction Values

TSMIP Stations	CWBSN-S13 Stations	Longitude (°E)	Latitude (°N)	κ_0 (s)	Station Correction
TTN014	CHK	121.3730	23.0978	0.020	−0.169
CHY089	CHN3	120.3643	23.0751	0.071	−0.340
CHY080	CHN5	120.6776	23.5973	0.077	−0.240
TTN052	ECL	120.9620	22.5960	0.045	0.087
HWA021	EHY	121.3299	23.5038	0.020	0.241
ILA050	ENA	121.7490	24.4263	0.042	−0.263
ILA025	ENT	121.5736	24.6378	0.015	0.018
HWA020	ESL	121.4415	23.8121	0.036	0.278
ILA067	NNS	121.3814	24.4374	0.049	−0.134
CHY077	SCL	120.2017	23.1735	0.078	−0.363
ILA052	TWC	121.8595	24.6082	0.005	0.261
HWA023	TWD	121.6048	24.0813	0.008	0.371
ILA051	TWE	121.6829	24.7180	0.024	0.071
TTN018	TWG	121.0799	22.8177	0.046	0.232
TCU088	TWT	121.1620	24.2495	0.011	−0.059
CHY076	WSF	120.2298	23.6364	0.075	−0.419

TSMIP, Taiwan Strong-Motion Instrumentation Program; CWBSN, Central Weather Bureau Station Network.

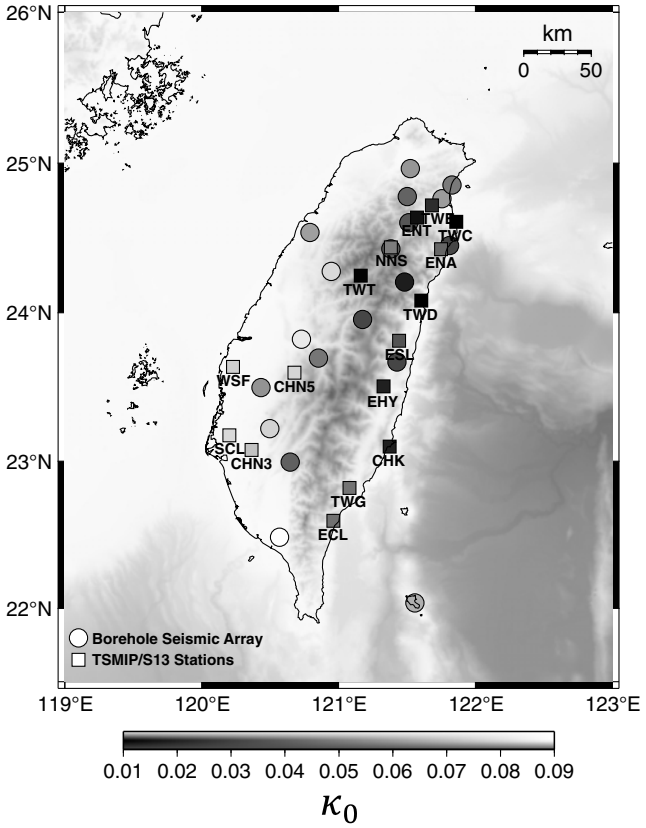

Figure 10. A map showing the estimated κ_0 values at all cosite Taiwan Strong-Motion Instrumentation Program (TSMIP) stations (squares) and 30 borehole seismic arrays (circles).

ing the weighted LS method in the second stage of inversion, which can significantly influence the accuracy of the κ_0 results. Figure 5 shows that the difference in κ_0-value between LS (first stage) and weighted LS (second stage) methods can reach ~20%. In addition, we also test the influence in estimating κ_0-value using epicenter and hypocentral distances. We found only a little difference in estimated κ_0-value. The κ_0-values estimated at all stations in this study are consistent with previous studies in Taiwan. In general, κ_0^s-values are found to be more than κ_0^b-values (Table 1). This is also in agreement with a few studies in the world carried out using borehole instruments. Then we conducted a series of regression analyses to investigate relationships between $\Delta\kappa_0$ and surface-to-borehole distance, and station correction and κ_0-value. Most notably, there is no good relation observed between $\Delta\kappa_0$ and surface-to-borehole distance (Fig. 9), other than geologic formations being primarily responsible for observed change in κ_0-values at different stations. These values can be useful for providing one of the most important site-effect parameters in GMPE and in the simulation process. These values can also be used as a reference for future studies.

Data and Resources

Strong-motion waveform records used in this study are obtained from the Taiwan Strong-Motion Instrumentation Program (TSMIP) and borehole seismic array, which are managed by the Central Weather Bureau (CWB) of Taiwan. All records are open to the public and can be obtained upon request from CWB. The current relocated earthquake catalog that included events between 1991 and 2014 used in this study can be obtained upon request from Y.-M. Wu. The Generic Mapping Tools software from Wessel and Smith (1998) was used in plotting part of the figures and is gratefully acknowledged.

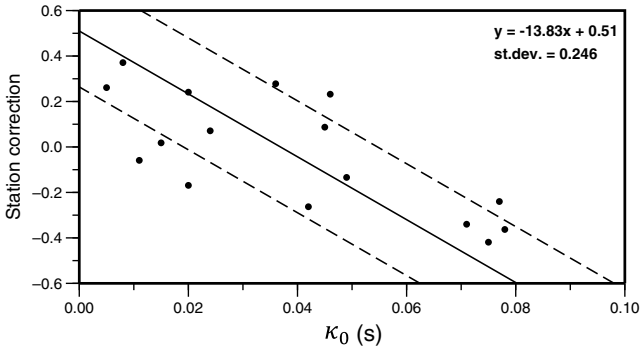

Figure 11. Regression for the relationship between the station correction and κ_0. The solid line shows regression line, whereas the two dashed lines indicate the range of one standard deviation (st. dev.).

Acknowledgments

The authors offer profuse thanks to the Ministry of Science and Technology (MOST) of Taiwan for funding the project, under which this study was carried out. The comments from two anonymous reviewers and Associate Editor Hiroshi Kawase helped improve the article. The authors are thankful to Cédric Legendre, whose constructive comments helped considerably in improving this manuscript.

References

Anderson, J. G. (1991). A preliminary descriptive model for the distance dependence of the spectral decay parameter in southern California, *Bull. Seismol. Soc. Am.* **81,** 2186–2193.

Anderson, J. G., and S. E. Hough (1984). A model for the shape of the Fourier amplitude spectrum of acceleration at high frequencies, *Bull. Seismol. Soc. Am.* **74,** 1969–1993.

Boore, D. M. (2003). Simulation of ground motion using the stochastic method, *Pure Appl. Geophys.* **160,** nos. 3/4, 635–676.

Campbell, K. W. (2009). Estimates of shear-wave Q and κ_0 for unconsolidated and semiconsolidated sediments in Eastern North America, *Bull. Seismol. Soc. Am.* **99,** 2365–2392.

Castro, R. R., L. Trojani, G. Monachesi, M. Mucciarelli, and M. Cattaneo (2000). The spectral decay parameter κ in the region of Umbria-Marche, Italy, *J. Geophys. Res.* **105,** 23,811–23,823.

Chen, K. P., C. Y. Wang, Y. B. Tsai, and W. Y. Chang (2013). A seismic structure study in the Kaoping Area, southwestern Taiwan, *Bull. Seismol. Soc. Am.* **103,** 306–316.

Cotton, F., F. Scherbaum, J. J. Bommer, and H. Bungum (2006). Criteria for selecting and adjusting ground-motion models for specific target regions: Application to Central Europe and rock sites, *J. Seismol.* **10,** 137–156.

Douglas, J., P. Gehl, L. F. Bonilla, and C. Gélis (2010). A κ model for mainland France, *Pure Appl. Geophys.* **167,** 1303–1315.

Fernández, A. I., R. R. Castro, and C. I. Huerta (2010). The spectral decay parameter kappa in northeastern Sonora, Mexico, *Bull. Seismol. Soc. Am.* **100,** 196–206.

Hanks, T. C. (1982). $f_{\max}$, *Bull. Seismol. Soc. Am.* **72,** 1867–1879.

Hough, S. E., and J. G. Anderson (1988). High-frequency spectra observed at Azna, California: Implications for Q structure, *Bull. Seismol. Soc. Am.* **78,** 692–707.

Hough, S. E., J. G. Anderson, J. Brune, F. Vernon, J. Berger, J. Fletcher, L. Haar, T. Hanks, and L. Baker (1988). Attenuation near Anza, California, *Bull. Seismol. Soc. Am.* **78,** 672–691.

Konno, K., and T. Ohmachi (1998). Ground-motion characteristics estimated from spectral ratio between horizontal and vertical components of microtremor, *Bull. Seismol. Soc. Am.* **88,** 228–241.

Ktenidou, O. J., C. Gélis, and L. F. Bonilla (2013). A study on the variability of kappa (κ) in a borehole: Implications of the computation process, *Bull. Seismol. Soc. Am.* **103,** 1048–1068.

Lai, T. S., H. Mittal, and Y. M. Wu (2016). 2012 seismicity quiescence in Taiwan a result of site effect artefacts, *Seismol. Res. Lett.* **87,** no. 4, doi: 10.1785/0220150260.

Lancieri, M., R. Madariaga, and F. Bonilla (2012). Spectral scaling of the aftershocks of the Tocopilla 2007 earthquake in Northern Chile, *Geophys. J. Int.* **189,** 469–480, doi: 10.1111/j.1365-246X.2011.05327.x.

Margaris, B. N., and P. M. Hatzidimitriou (2002). Source spectral scaling and stress release estimates using strong-motion records in Greece, *Bull. Seismol. Soc. Am.* **92,** 1040–1059.

Mittal, H., and A. Kumar (2015). Stochastic finite-fault modeling of M_w 5.4 earthquake along Uttarakhand–Nepal border, *Nat. Hazards* **75,** 1145–1166.

Mittal, H., Y. M. Wu, D. Y. Chen, and W. A. Chao (2016). Stochastic finite modeling of ground motion for March 5, 2012, M_w 4.6 earthquake and scenario greater magnitude earthquake in the proximity of Delhi, *Nat. Hazards* 1–24, doi: 10.1007/s11069-016-2236-x.

Motazedian, D., and G. M. Atkinson (2005). Stochastic finite-fault modeling based on dynamic corner frequency, *Bull. Seismol. Soc. Am.* **95,** 995–1010.

Oth, A., D. Bindi, S. Parolai, and D. Di Giacomo (2010). Earthquake scaling characteristics and the scale-(in) dependence of seismic energy-to-moment ratio: Insights from KiK-net data in Japan, *Geophys. Res. Lett.* **37,** L19304, doi: 10.1029/2010GL044572.

Oth, A., D. Bindi, S. Parolai, and D. Di Giacomo (2011). Spectral analysis of K-NET and KiK-net data in Japan, part II: On attenuation characteristics, source spectra, and site response of borehole and surface stations, *Bull. Seismol. Soc. Am.* **101,** 667–687.

Papageorgiou, A. S., and K. Aki (1983). A specific barrier model for the quantitative description of inhomogeneous faulting and the prediction of strong ground motion. I. Description of the model, *Bull. Seismol. Soc. Am.* **73,** 693–722.

Purvance, M. D., and J. G. Anderson (2003). A comprehensive study of the observed spectral decay in strong-motion accelerations recorded in Guerrero, Mexico, *Bull. Seismol. Soc. Am.* **93,** 600–611.

Tsai, C.-C. P., and K.-C. Chen (2000). A model for the high-cut process of strong-motion accelerations in terms of distance, magnitude, and site condition: An example from the SMART 1 array, Lotung, Taiwan, *Bull. Seismol. Soc. Am.* **90,** 1535–1542.

Van Houtte, C., S. Drouet, and F. Cotton (2011). Analysis of the origins of κ (kappa) to compute hard rock to rock adjustment factors for GMPEs, *Bull. Seismol. Soc. Am.* **101,** 2926–2941.

Wessel, P., and W. H. F. Smith (1998). New improved version of Generic Mapping Tools released, *Eos Trans. AGU* **79,** no. 47, 579.

Wu, Y. M., C. H. Chang, L. Zhao, J. B. H. Shyu, Y. G. Chen, K. Sieh, and J. P. Avouac (2007). Seismic tomography of Taiwan: Improved constraints from a dense network of strong-motion stations, *J. Geophys. Res.* **112,** no. B08312, doi: 10.1029/2007JB004983.

Wu, Y. M., C. H. Chang, L. Zhao, T. L. Teng, and M. Nakamura (2008). A comprehensive relocation of earthquakes in Taiwan from 1991 to 2005, *Bull. Seismol. Soc. Am.* **98,** 1471–1481, doi: 10.1785/0120070166.

Department of Geosciences
National Taiwan University
Taipei 10617, Taiwan
himanshumitt10@gmail.com

Manuscript received 4 January 2016;
Published Online 14 June 2016